Low-temperature deposition of self-cleaning anatase TiO2 coatings on polymer glazing via sequential continuous and pulsed PECVD

Benjamin Dey, Simon Bulou, William Ravisy, Nicolas Gautier, Mireille Richard-Plouet, Agnès Granier, Patrick Choquet

Low-temperature deposition of self-cleaning anatase TiO_2 coatings on polymer glazing via sequential continuous and pulsed PECVD

DEY Benjamin [1], BULOU Simon [1,*], RAVISY William [2], GAUTIER Nicolas [2] , RICHARD-PLOUET Mireille [2], GRANIER Agnès [2], CHOQUET Patrick [1]

[1]Luxembourg Institute of Science and Technology, Materials Research and Technology Department, 5 Avenue des Hauts-Fourneaux, L-4362, Esch-sur-Alzette, Luxembourg

[2]Institut des Matériaux Jean Rouxel (IMN), Université de Nantes, CNRS 2 rue de la Houssinière, BP 32229 44322, Nantes, France

*corresponding author: Dr. Simon BULOU, simon.bulou@list.lu

Mr. Benjamin DEY, benjamin.dey@list.lu

Dr. Simon BULOU, simon.bulou@list.lu

Dr. William RAVISY, william.ravisy@cnrs-imn.fr

Mr. Nicolas GAUTIER, nicolas.gautier@cnrs-imn.fr

Dr. Mireille RICHARD-PLOUET, mireille.richard@cnrs-imn.fr

Dr. Agnès GRANIER, agnes.granier@cnrs-imn.fr

Dr. Patrick CHOQUET, patrick.choquet@list.lu

Abstract:

Photocatalytic properties of semiconductor materials, studied now for decades, represent huge potentialities as environmentally friendly self-cleaning surfaces. Up to now, inexpensive and non-toxic TiO_2-based photocatalysts remain the most interesting solution from practical and industrial point of view. Nevertheless, obtaining titania surface in its anatase phase, polymorph presenting the best photocatalytic property, usually requires high temperature. Hence, anatase containing self-cleaning titania coatings are still limited industrially to inorganic glazing. In this article, we present an innovative sequential deposition method using continuous and pulsed plasma enhanced chemical vapour deposition enabling the deposition of anatase photocatalytic thin films at substrate temperature below 60 °C. The morphology and crystalline structure of the TiO_2 thin films deposited in both pulsed and continuous modes are investigated. Then, the combination of these two methods used sequentially successfully led to the deposition of self-cleaning TiO_2 coatings on thick polycarbonate substrates without alteration, opening a new way for the deposition of photocatalytic coatings on thermolabile substrates such as organic glazing or lenses.

KEYWORDS : pulsed plasma; anatase TiO_2; low temperature PECVD; Polycarbonate; photocatalysis; self-cleaning coatings

1.1 Introduction

Photocatalysis is an advanced oxidative process involving light, a catalyst, and a pollutant (organic compounds, industrial dyes, viruses, bacteria, and so on). From an environmental perspective, this reactive pathway is often considered as a potential green alternative to conventional wastewater treatments (sedimentation, filtration, or ozonation) [1] as it can lead to the absolute mineralization of the pollutant and not only to its separation from the medium [2], [3]. As a more practical application, TiO_2 coated glazing (Pilkington Aktiv, Kastus) display a very good self-cleaning ability enabling to cut down the maintenance and cleaning costs in term of both money and chemical wastes [1]. So far, many semiconductors have proven their abilities to effectively take part to photocatalytic reactions (CdSe, Fe_2O_3, WO_3, Bi_2WO_6, $BiVO_4$, CdS, ZnO, TiO_2) but up to now, TiO_2 and TiO_2-based photocatalysts remain the favoured candidates [4]. Intrinsic properties of TiO_2, namely its low toxicity, low price, significant photocatalytic activity and high chemical, mechanical and photo-stability, justify the prominent place these systems have and will take in today's and tomorrow's photocatalytic applications. Nonetheless, few intrinsic impediments are still slowing down its industrial expansion. On the one hand, its band gap, around 3.2 eV, restricts TiO_2 light absorption to the extreme blue tail and UV part of the solar spectrum which represents less than 5% of the solar energy shining on Earth surface [5]. And on the second hand, the most photocatalytic polymorph of TiO_2 (anatase), usually requires high temperature (>150 °C) either during the synthesis or a post annealing treatment, preventing thus the deposition on thermolabile substrates such as many polymers.

Few years ago, TiO_2 nanopowders were largely investigated for photocatalytic applications as they provide high surface/volume ratio and by consequence, the most promising photocatalytic efficiency. Nevertheless, the use of nanoparticles presents serious impediments. In particular for wastewater treatment, the post recovery of TiO_2 powder from wastewater remains mandatory (toxicity of TiO_2 nanoscale suspension [6], [7], [8], [9]), expensive and laborious

[10]. To overcome these issues, well adherent and stable TiO_2 coatings need to be developed before any process upscale. As a matter of fact, wet-chemistry route, already led to dispersed anatase nanopowder synthesis < 100°C via multiple steps processes or long aging treatment (7-14 days at 40°C [11], 2 days 60°C [12]). But, up to now, the main route to obtain anatase TiO_2 on polymer's surface still relies on immobilization of these crystalline powders via a reasonable heat treatment [13]. However, the adhesion between the polymer and the crystalline catalyst might not be good enough and therefore may jeopardize the mechanical stability of the polymer-supported photocatalyst [9], [14], [15], [16]. Anyhow, it appears that appropriate plasma pre-treatment of the polymeric substrate could increase the adhesion between TiO_2 powders and polyethylene and polypropylene surfaces [17]. Thus, the development of processes allowing, in a reasonable time frame, to deposit highly photocatalytic TiO_2 crystalline layer with good adhesion on polymeric substrate is a cornerstone of its further expansion at an industrial scale. Plasma Enhanced CVD technology has shown its ability to synthesize TiO_2 anatase thin films at substrate temperature significantly lower than thermal CVD (below 150 °C whereas T_{sub} > 200°C are usually required in CVD processes) thanks to the reactive plasma species produced. But most of the time, the deposited materials remain amorphous below 150°C [18]. Hence, several experimental investigations have been pursued to get a well-crystallized titania layer at low substrate temperature. Among them, we can cite few articles where process parameters such as the Ti precursor (Titanium tetrachloride $TiCl_4$,Titanium tetraisopropoxide TTiP, Tetrakis(dimethylamido)titanium(IV) TDMAT, Titanium ethoxide $Ti(OEt)_4$), precursor dilution [19,20], [21], plasma gas composition [22] (Ar, O_2, H_2, N_2 and mixtures), plasma configuration (direct or remote [23]), excitation frequency [24] (Low frequency [25], Radiofrequency and Microwaves [26]), power input [27], substrate biasing [28], epitaxial growth [29], [30], [31] and even samples thickness [32], [33], [34], [35], have been explored. More recently, the way that the plasma discharge is assisting the CVD process has been studied to tailor the films properties and quality. Hence, pulsed waves plasma have been investigated

to further decrease the temperature of the coatings while maintaining a partially crystallized structure [36]. In a recently published paper [37], we demonstrated the great ability of pulsed wave (PW) Electron Cyclotron Wave Resonance (ECWR) plasma technology to deposit crystalline TiO_2 at low temperature. Based on fine tuning of the duty cycle ($DC = T_{Plasma\ On}/(T_{Plasma\ On} + T_{Plasma\ Off})$) and the gas composition, one could deposit anatase TiO_2 at $T_{sub\ max} < 120°C$ with a growth rate of 10 $nm.min^{-1}$. Interestingly, the thickness deposition rate appears slightly higher in pulsed deposition mode by comparison with a continuous wave plasma. This suggests that at a pulse frequency of 10 kHz, the film deposition is occurring during both periods (T_{On} and T_{Off}), implying a superposition of different growth mechanisms.

To better understand the deposition mechanisms at stake in pulsed discharge process, we investigate in this article the morphology and the crystalline structure of films deposited with both plasma modes, a continuous wave mode with a discharge power of 500 W and a pulsed wave mode (DC = 50%; f = 10 kHz) with a crest power of P_{Crest} 500W. These investigations pointed out that, when using pulsed plasma, the substrate temperature can be precisely tuned and kept low but the appearance of anatase nuclei is significantly delayed. Thus, we propose a two steps deposition method, combining a continuous waves plasma step (CW) and a pulsed wave plasma step (PW) successively. This Sequential Deposition mode (SD) using our ECWR PECVD process has enabled the deposition of photocatalytic anatase TiO_2 below 60 °C. The practical relevance of this process is finally assessed with the deposition of photocatalytic anatase TiO_2 coating on thick polycarbonate sheets (2 mm). The coated polycarbonate exhibits an important and rapid self-cleaning effect, thus opening the way for elaboration of photocatalytically active surfaces on a wide range of thermolabile substrates such as low melting point polymers.

2.1 Experimental

1.1. Plasma Enhanced Chemical Vapour Deposition process

The experimental set-up (Figure 1a) used was equipped with a low-pressure radiofrequency (13.56 MHz) **E**lectron **C**yclotron **W**ave **R**esonance **P**lasma **E**nhanced **C**hemical **V**apour (ECWR-PECVD) source (COPRA DN 200 CF, CCR Technology) [38]. This plasma source consists in a single turn RF driven electrode and a low transverse static magnetic field ($|\vec{B}|\approx$ tens of Gauss) allowing the creation of high-density plasma even at low pressure (< 10^{-3} mbar) [39]. A grounded tungsten grid at the exit of the source allows confining the plasma inside the source. A quasi-neutral plasma beam (composed of electron, ions and neutral species) diffuses out through the extraction grid and interacts in the deposition chamber with the titanium precursor. Titanium (IV) tetraisopropoxide (TTiP, $Ti[OCH(CH_3)_2]_4$, 97 wt%, Sigma-Aldrich) vapour is injected into the deposition chamber with a bubbler system at room temperature and using argon as carrier gas. The pressure in the bubbler was maintained between 4.5 and 5.1 mbar (TTiP saturated vapour pressure = 0.13 mbar @ 23°C). Ar carrier gas flow was fixed at 7 sccm, thus corresponding to 0.16 sccm of TTiP introduced into the deposition chamber by means of a dispersal ring between the ECWR plasma source and the substrate holder. The ECWR plasma source was fed with a mixture of Ar and O_2 with a flowrate of 12.5 and 37.5 sccm, respectively. The total pressure in the chamber was set at 5.10^{-3} mbar, thanks to a throttle valve installed between the deposition chamber and the turbomolecular pump. In this work, TiO_2 films were deposited on intrinsic silicon substrate ((100), thickness = 280 µm, single side polished) and on thick polycarbonate (PC) sheets (2 mm, GoodFellow). The substrate temperature was measured thanks to a K-thermocouple taped on the top of each substrate. The ECWR plasma source can work both in continuous and pulsed modes. For this study, both modes were used, and a frequency of f = 10 kHz was applied for the pulsed mode.

Although the set up descibed in a previous work enabled to deposit anatase TiO_2 at $T_{sub\ max}$ < 120°C [37], it has been sligthly tweaked in the perspective of lowering the deposition temperature even further. As such, copper substrate holder was used and temperature evolutions were compared with the one obtained previously on a stainless steel substrate holder. The evolutions of the substrate temperature under 500 W CW (red) and 500 W pulsed with a duty cycle of DC = 50% (green) are displayed in Figure 1b. From a manufacturing point of view, this statement is very important as it demonstrates the possibility of this plasma source to synthesize an anatase phase surface at really low temperature (<100 °C) and opens the possibility to synthesize photocatalytic surfaces on thermolabile substrates.

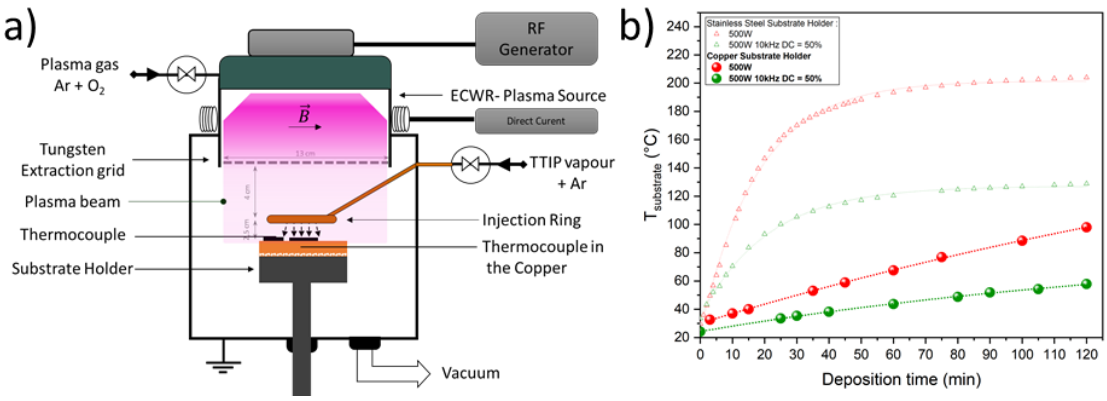

Figure 1 : ECWR set-up (a) and substrate temperature as a function of deposition time under 500W CW (red) and 500W pulsed DC = 50% 10 kHz (green) for two different substrate holder made out of stainless steel (triangles) and copper (spheres) (b)

1.2. Structural Characterization

The surface morphology was investigated by Scanning Electron Microscopy (SEM) performed using a Hitachi SU-70 Field Emission-SEM. The crystalline structure of the films was analysed using a Renishaw inVia micro-Raman spectrometer. A laser beam (λ=532 nm, P=2.6 mW) was focused on a 1 µm² area on the top surface of the coating. For all the coatings analysed, Si characteristic peak of the wafer could be observed at 521 cm^{-1}, therefore we assume all the coating was scanned.

The crystalline structure and preferential orientation of crystallites have been investigated through X-ray Diffraction (XRD) using a Bruker D8 Advance diffractometer (Cu Kα radiation) in Bragg-Brentano geometry (2θ = 22 to 64°, step 0.03°, acquisition for 10 h). TiO_2 anatase peaks were attributed thanks to JCPDS file number 89-4921. TiO_2 thin film thickness was determined by SEM on cross sections In addition, FIB prepared cross sections of two representative as-deposited TiO_2 coatings (CW and PW) were investigated using transmission electron microscopy (S/TEM Themis Z G3, 300kV, Thermo Fisher Scientific). Selected Electron Area Diffraction (SAED) was conducted along the thickness to assess whether the different regions of the films were crystalline or not.

1.3. Functional properties investigations

The photocatalytic activity of the as-deposited TiO_2 films was evaluated by measuring Methylene Blue (MB) degradation in aqueous solution under 2 mW/cm² UV exposure (Herolab UV-8 SL, 365 nm, 16 W) and solar simulator (LCS-100, Oriel Instruments). The samples were immersed in aqueous MB solution (1 µmol.L^{-1}) and stored in dark into a black box overnight before being exposed to the light source so the adsorption/desorption equilibrium could reach a steady state. The UV lamp was positioned at 10 cm above the samples, corresponding to 2 mW/cm² irradiance on the samples surface (irradiance measured by a radiometer RM 12, Opsytec Dr.Gröbel). MB concentration of the solution was then quantified by measuring its absorbance at 665 nm (UV-Visible Spectrophotometer, Tecan Infinite M1000 Pro). The photodegradation kinetic was determined through the monitoring of absorbance decrease as a function of UV illumination duration. The concentration of the MB solution was set at 1 µmol.L^{-1} so we assumed that the active sites on the TiO_2 surface were in excess compared to MB molecules. Therefore, a pseudo-first order kinetic is a relevant model to fit the data and extract the degradation constant k (h^{-1}).

$$[MB]_t = [MB]_0 * e^{-kt}$$

3.1 Results and discussion

In a former article, it was established that, providing a fine tuning of plasma deposition parameters, TiO_2 thin films growth occurs following a transition from amorphous to anatase along the thickness [37]. During these studies, the ECWR plasma source has shown its ability to readily deposit anatase layers with high power input [38] and at a high deposition rate [37] (≈10 $nm.min^{-1}$). Also, it is worth mentioning that the proposed process provides very good uniformity of coating thickness (+/- 5 % thickness on 5x5 cm^2 surface) and excellent crystalline homogeneity. Whereas substrate temperature is a major factor to tune the layers from amorphous to anatase structure, it appeared that thanks to a fine tuning of the plasma pulsing parameters, it is possible to favour anatase crystal germination at lower temperature (<120°C). In the following article, we focus on the feasibility to synthesize anatase TiO_2 films by ECWR at very low temperature (below 80°C).

To progress in the global understanding of TiO_2 growth mechanisms in this pulsed plasma conditions on low substrate surface temperature, we have then carried out a study of the TiO_2 morphology and crystallinity obtained for CW and PW mode. To do so, coatings obtained with different deposition duration for both modes were deposited, then hereafter, analysed thoroughly by SEM (Figure 2), Raman spectroscopy, X-ray diffraction (XRD), Transmission Electron Microscopy (TEM) and Selected Area Electron Diffraction (SAED) analysis.

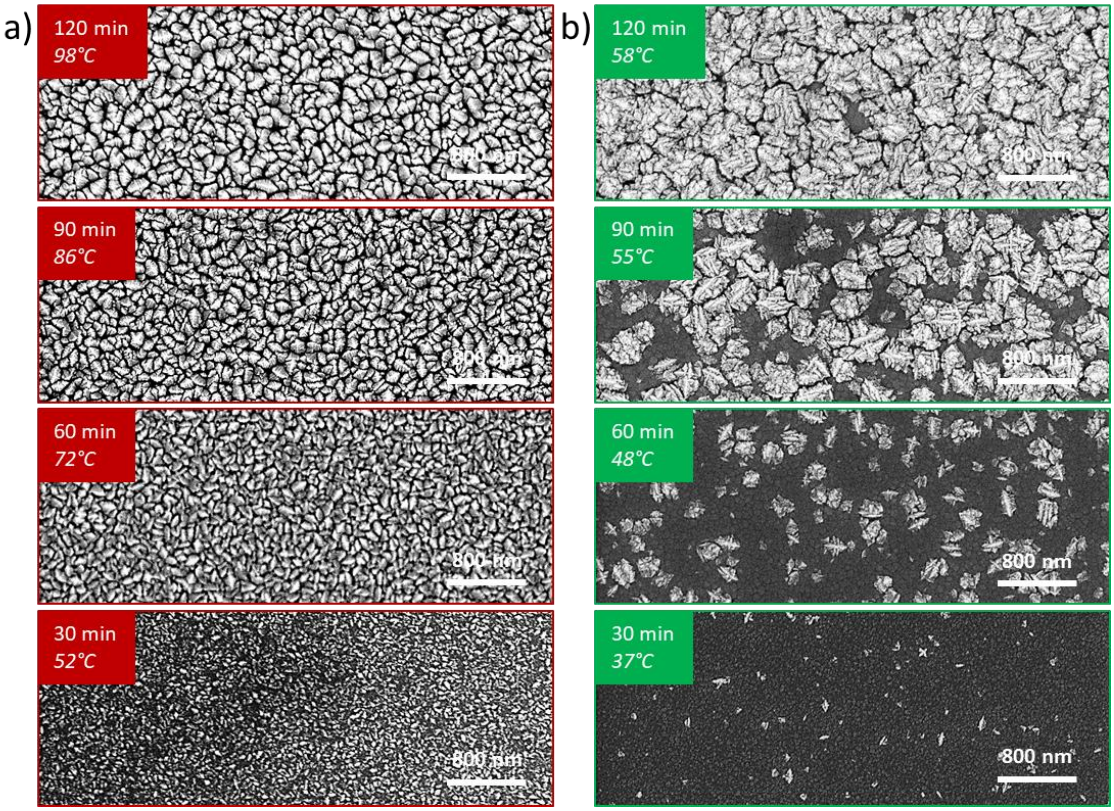

Figure 2 : TiO_2 SEM topviews micrographs obtained for different deposition time using CW process (a) and PW process (b)

According to SEM top view micrographs (Figure 2), noticeable differences clearly appear between TiO_2 coatings deposited with continuous (CW) and pulsed (PW) plasma, in particular regarding the density and size of large bright islands visible on the surface. Indeed, coatings synthesised using CW plasma (Figure 2a) already exhibit white nuclei sprouting all over the surface after 30 min deposition, this may correspond to the anatase coalescence stage. Also, from these surface observations and considering that the coating is elaborated with this plasma process at low substrate temperatures, supported by our previous work [40]we propose that these brighter islands are associated to the top of a columnar coating. This statement is verified with TEM observations of FIB prepared cross-sections of thick TiO_2 coatings (Figure 3). In addition, several TEM analysis of TiO_2 thin films deposited using the same process but with different experimental conditions (unpublished results) evidenced that bright grains visible on the topmost surfaces using SEM are the top of crystalline columns. This growth mechanism

may be in agreement with the Kolmogorov model of growth for crystalline TiO_2 during its coalescence step [26]. After 60 min deposition, one can see well-defined top faceted columns spread all over the coating surface. Besides, the surface of TiO_2 layers synthesised using PW (f =10 kHz, DC = 50%, P_{crest} =500W), (Figure 2b) shows only few white sparse features dispersed in the dark-contrasted sublayer after 30 min deposition. This may indicate that the start of the nucleation phase using PW is delayed compared to CW. After 60 min deposition time using PW, the already existing nuclei enlarged, and new ones start popping out of the dark-contrasted sublayer. After 120 min of PW deposition, the surface appears almost entirely covered. In order to further study the thin film growth mechanism, and more particularly, the structure transition along the thickness, TEM and SAED observations were achieved on FIB prepared cross sections of 900 nm thick (2 hours deposition) TiO_2 films deposited in both modes (Figure 3).

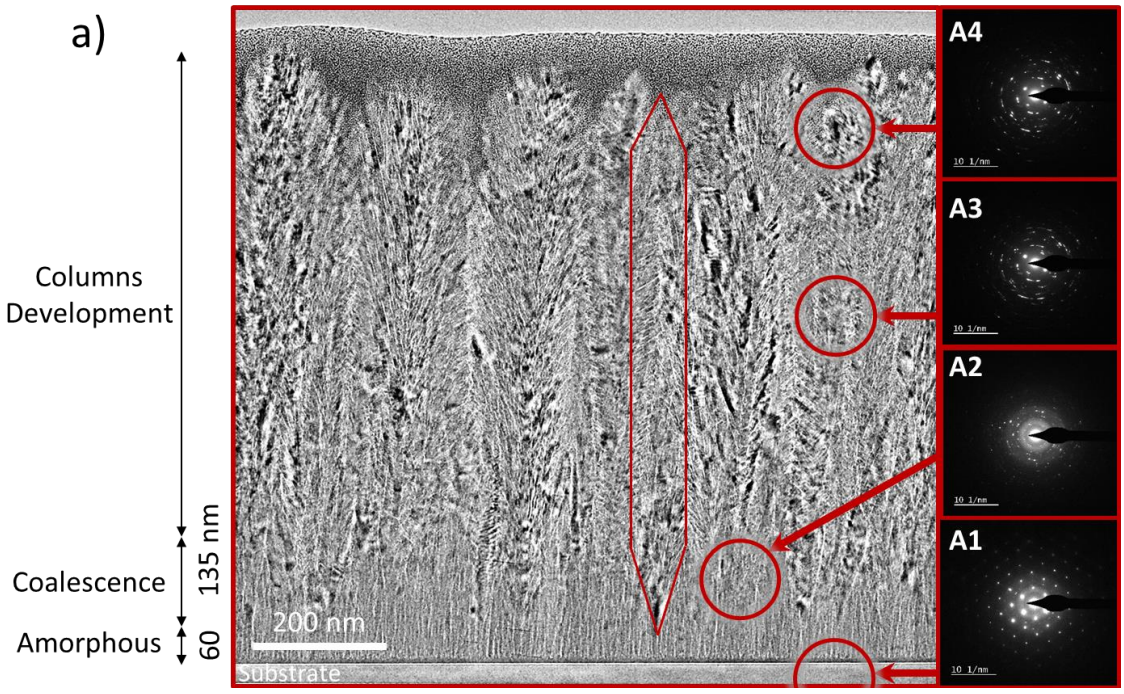

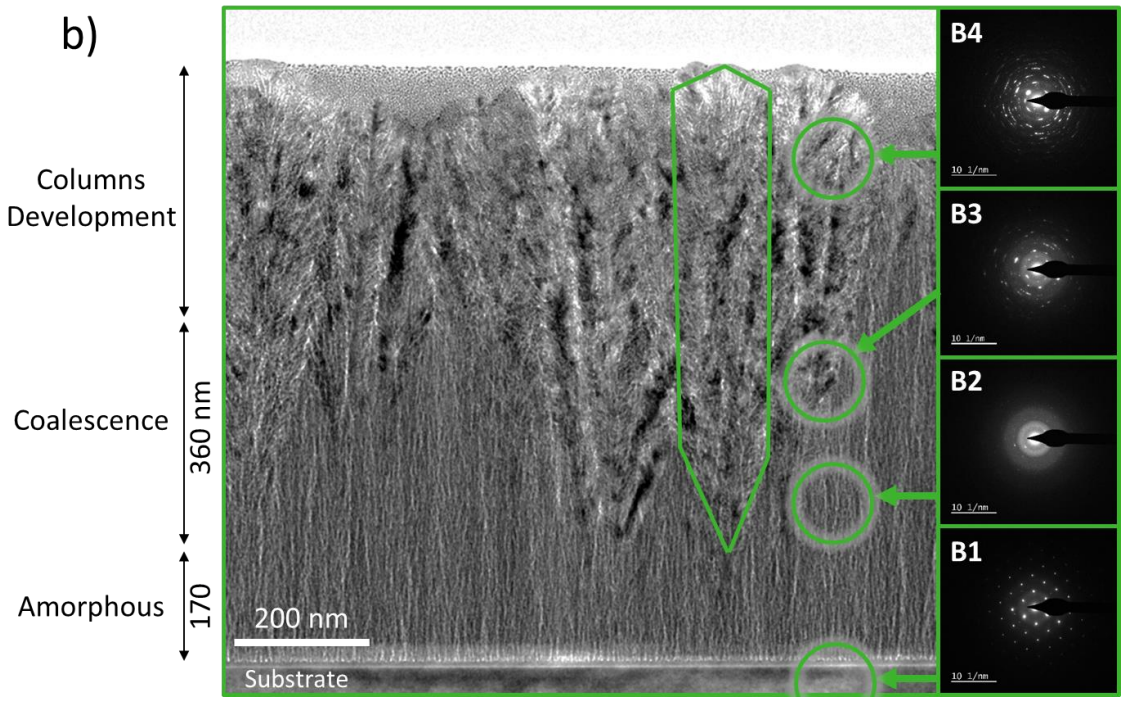

Figure 3 : TEM and SAED analysis of 120 min CW (a) and PW (b)

Figure 3 displays SAED measurements carried out on 4 different areas for CW (Figure 3a) and PW (Figure 3b) coatings. For CW deposited coating, SAED of area A1 corresponds to Si substrate. SAED in the first tens of nanometre of deposited coating, corresponding to the transition fibrous/columnar, revealed characteristic features of both amorphous and anatase TiO_2. Upper in the layer, SAED of areas A3 and A4 (approximatively at 500 nm and 800 nm from the Si surface respectively), present electronic diffraction signature corresponding to polycrystalline anatase phase. Regarding the PW deposited coating (Figure 3b), area B1 is clearly representative of Si substrate. When pointing at the fibrous dark-contrasted matrix (B2) no crystalline structure is evidenced by SAED confirming the amorphous nature of this structure. Upper in the layer (B3 and B4), SAED analysis reveals evidences of titania crystallised under anatase phase.

Thus, as evidenced from other characterisation techniques, one can observe two regions in the cross-view. Also, SAED evidenced that the fibrous dark structure at the interface Substrate/TiO_2 is amorphous whereas in the larger bright columns arising at the surface, the

electron diffraction patterns are typical for TiO_2 anatase variety. It is worth mentioning that the amorphous TiO_2 layer is thicker in PW than in CW mode (170 and 60 nm respectively). Similarly, the transition layer (coalescence layer) is thicker in PW than in CW mode (360 nm and 135 nm respectively). Besides, the width of the crystalline columns (measured and averaged on several TEM images) for CW mode is around 80 nm whereas the column width obtained in PW appears bigger (140 nm). These differences revealed that in the case of CW, numerous anatase nuclei are formed and the coalescence stage is quickly reached leading to a competitive growth of the columns. Whereas in PW mode, due to the lower density of anatase nuclei, this competitive growth is limited. This concept of coalescence thickness (i.e., thickness once coalescence is achieved) for TiO_2 grown by pulsed and continuous waves ICP-PECVD has been evidenced in another work thanks to in-situ ellipsometry [41]. The coalescence thickness value may vary depending on the plasma source configuration, titanium precursor flow and RF power applied.

In order to confirm that the bright structures emerging out of the dark contrasted matrix are associated to the density of anatase phase, semi quantitative analysis of TiO_2 films were carried out by Raman spectroscopy and are reported in Figure 4a (CW) and b (PW).

Since the laser probe interacts with the total thickness of each TiO_2 coating (evidenced by the Raman diffusion peak observation of Si substrate at 512 cm^{-1} for all analysed coatings) and because the focalisation of the laser is similar (focalisation on the top-most surface), it can be assumed that the area of the Raman diffraction peaks is representative of the total quantity of anatase embedded in the coating. Figure 4c represents the integrated area under the main characteristic peak of anatase (Eg 144 cm^{-1}) for CW and PW synthesis. For CW deposited coatings, a linear increase of anatase amount as a function of the layer thickness is observed from 200 nm. This implies that after a certain thickness, the quantity of new anatase crystals synthesised is constant with time. On the contrary, PW mode needs a period before a regular increase of anatase amount occurs. Consequently, for a similar deposition duration, the overall

amount of anatase synthesized in coatings deposited in PW mode is lower than for the coatings deposited in CW mode. Also, according to Figure 4c, it can be reported that the transition between amorphous to anatase starts after a film thickness of 300 nm and spreads up, at least, to 900 nm for the films deposited in PW mode. This statement is in good agreement with SEM and TEM micrographs, which indicated that, between 30 and 120 min deposition, crystalline nucleation, coalescence, columns formation and columns development were occurring concomitantly. More interesting, this high density of anatase on topmost surface is obtained at a substrate temperature not exceeding 60°C thanks to PW mode. On the contrary, CW deposition process does not offer such flexibility. Raman diffusion spectra also provided a qualitative information about the size of crystallized grains incorporated into the layers [42]. The evolution of Full Width Half Maximum (FWHM) of the E_g mode peak at 144 cm^{-1} is depicted in Figure 4Figure 5d. One can see that the FWHM of CW deposited samples is lower than these for PW mode for the same deposition time, revealing bigger anatase crystallites size in the CW deposition condition. Besides, the FWHM decreases in both modes with increasing deposition time, indicating that the crystallite size increases as the films grew thicker.

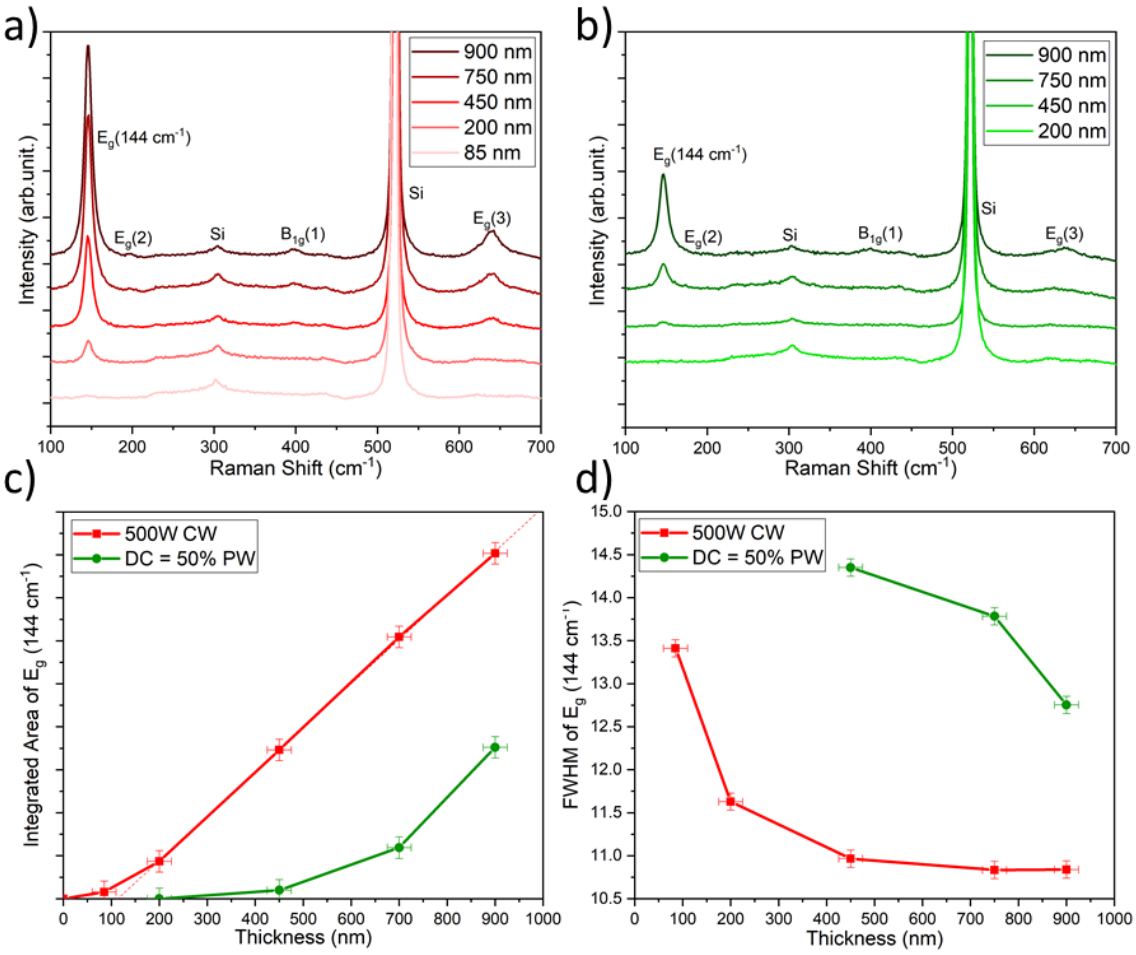

Figure 4 : TiO_2 coatings Raman spectra for CW (a) and pulsed deposition (b) and their integrated area under Lorentzian fit for peak at 144 cm^{-1} (c) and FWMH of 144 cm^{-1} (d)

To complete, XRD analysis of different coating thicknesses deposited in both modes also confirmed the crystallinity evolution as a function of deposition time. In addition, it also enlightens strong differences in terms of preferential crystalline orientation (Figure 5).

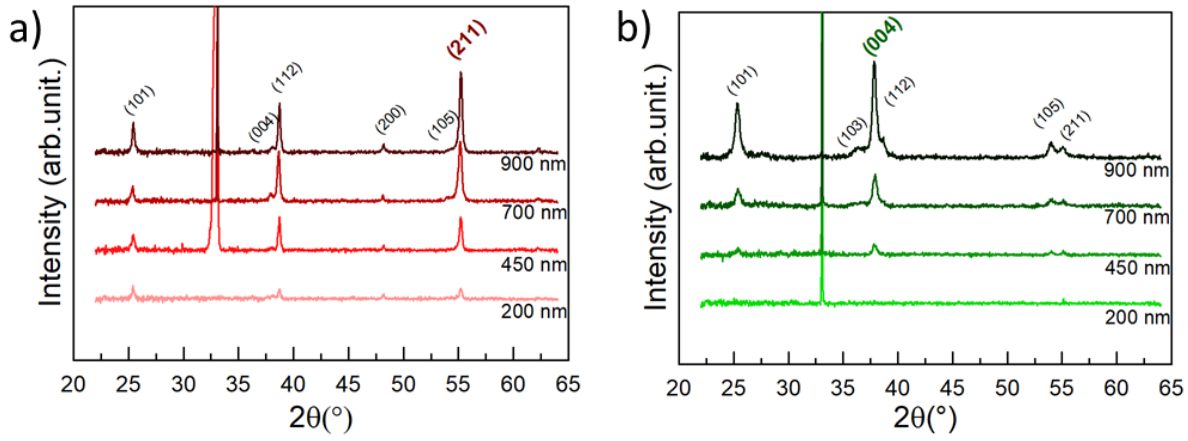

Figure 5 : XRD spectra of samples deposited in CW (a) and PW (b) for different thicknesses

Indeed, several diffraction peaks typical of anatase variety (according to JCPDF file N°89-4921) are detected. The detected diffraction peaks are located at 2θ equal to 25.3° 36.2° 37.7° 38.7° 48.2° 54° and 55.1° corresponding to the indexations of anatase planes (101) (103) (004) (200) (105) and (211) respectively. It is worth noticing that (200) plane is only observed for CW mode deposited coatings whereas (103) plane only appears for the 900 nm thick TiO_2 film deposited in PW mode. Compared to the expected intensities for a randomly oriented powder, some variations are observed and are attributed to preferential growth along given directions. Indeed, by calculating the Lotgering factors for the different deposition conditions, it is possible to illustrate the difference between the two modes as a function of the coating thickness and to detect possible preferred orientation degree of thin films, along the perpendicular direction to the substrate [43]. These factors for all samples are presented Figure 6. (211) and (004) crystallographic planes are identified as preferential facets for CW and PW respectively. Indeed, for the 900 nm thick films, the Lotgering factor was evaluated around $L_{(211)} = 0{,}40$ (CW) and $L_{(004)} = 0{,}40$ (PW).

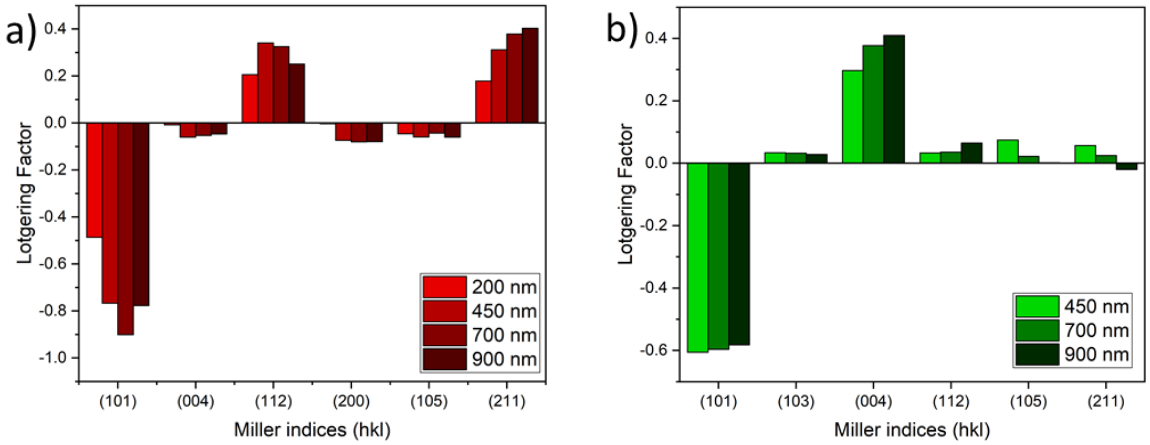

Figure 6 : Lotgering Factor calculated for TiO_2 samples deposited by ECWR PECVD in Continuous Wave (a) and Pulsed mode (b)

Amongst various features that have a significant role in photocatalytic activity (PCA), the impact of the crystallographic planes exposed to the pollutant have attracted a lot of attention [44,45], [46], [47]. It is here interesting to point out that PW deposited samples offer a preferential orientation for (004) planes which is one of the {001} plane family. The reactivity of the {001} planes family is attributed to two main factors. The main one is their high surface energy and the other is a high density of unsaturated five-fold coordinated Ti centers that provide acidic centres for dissociative adsorption of H_2O molecules [48].

Nevertheless, the (001) planes are usually swallowed up by others more stable such as the facets {101} as the film grows thicker because of its higher surface energy [49] (energies (γ) of main crystallographic planes observed in the literature are reported to be classified as follows $\gamma_{\{111\}}$ (1.61 $J.m^{-2}$) > $\gamma_{\{110\}}$ (1.09 $J.m^{-2}$) > $\gamma_{\{001\}}$ (0.9 $J.m^{-2}$) > $\gamma_{\{010\}}$ (0.53 $J.m^{-2}$) > $\gamma_{\{101\}}$ (0.44 $J.m^{-2}$)). This behaviour is generally detrimental for heterogeneous catalytic processes because higher crystal surface energy enables a better water and organic compound adsorption therefore enhancing their photodegradation kinetic [49]. Consequently, PW deposited samples present a favourable highly active plane of anatase crystal thanks to their preferential orientation.

Besides, it has been reported that (101) and (001) planes displayed reductive and oxidative sites respectively. Thus, having both exposed facets to the external medium can promote the natural separation of photogenerated charges [44]. Hence, anatase TiO_2 layers deposited in PW mode presented in this article offers the advantage of containing a mix of highly reactive planes.

Thus, for the synthesis of crystalline TiO_2 layers for photocatalytic applications, both plasma modes offered advantages and drawbacks. On one hand, 500 W delivered continuously to the gas discharge (CW) brought up crystalline germination at the early stage of growth, namely at 60 nm for the used experimental conditions (i.e., after 5/6 min). Nonetheless, the increase in temperature was linear with time with a slope of 0.57°C/min and jumped from nearly room temperature to 100°C within two hours, which may be too high for many polymers with rather low glass temperature transition. On the other hand, PW allows keeping substrate temperature

below 60°C but may take up to three times longer to start to initiate a sparse anatase nucleation sites. Regarding the crystallization mechanisms of CVD vacuum processes, other authors have also reported on an incubation layer before triggering any germination of crystalline sites. This intermediate amorphous layer is not only detected during the growth of crystalline TiO_2 but also for various inorganic coatings. To circumvolve this inconvenience, different authors have proposed process adaptations. Beato *et al.* applied a SiF_4 – He plasma pretreatment to suppress the intermediate amorphous layer of their µc-silicon films [50]. Nie *et al.* looked deeper into the thickness dependence crystallization of HfO_2 and Al_2O_3 by Atomic Layer Deposition (ALD) revealing a critical thickness and temperature triggering the amorphous to crystalline transition [51]. Another example was given by Kukli *et al.* [52] who deposited zirconia layers at various thicknesses and temperatures. It turned out that this critical thickness could be lowered from hundreds down to few nanometers by a severe increase (100 to 600°C) of substrate temperature. Hence, for these CVD or ALD processes, the main path to reduce or even suppress the growth of the amorphous intermediate layer is driven by an increase of the substrate temperature. However, Borrás *et al.* who also worked on the synthesis of TiO_2 by PECVD, have shown that in addition to temperature, an increase of the oxygen concentration in the discharge can accelerate the amorphous to anatase transition [53]. Also, Yasuda *et al.* demonstrated the great interest of seeding anatase crystal germs to quickly achieve the growth of complete anatase film at low temperature [29]. For that, they used the combination of an anatase bottom layer plus an acceleration voltage of 600 V to the ionic oxygen species impinging the substrate. The amorphous intermediate layer was suppressed and the homo epitaxial growth readily occurred at room temperature by using the so-called "Oxygen-ion-assisted Reactive Evaporation technique". Thus, it is possible to grow anatase TiO_2 at room temperature under vacuum process providing an appropriate ionic energy/flux and bottom seeding layer. However, the current cornerstone of such approach lays in the high temperature required to grow the appropriate crystalline bottom-most layer.

In the last part of this study, we hereafter propose an original approach to deposit anatase coating films while keeping the substrate temperature under 60°C. To do so, the process will combine the two deposition regimes in order to take advantage of both plasma modes. Hence, a sequential deposition (SD) regime composed of two different steps is proposed in the following section. First, a bottom-most layer is deposited in continuous mode, to take advantage of the fast and efficient anatase nucleation ability of the CW mode. Second, the growth of the anatase containing nuclei is further achieved by a pulsed plasma process to lower the substrate temperature increase induced by the plasma. The results regarding this sequential process are summarized in Figure 7.

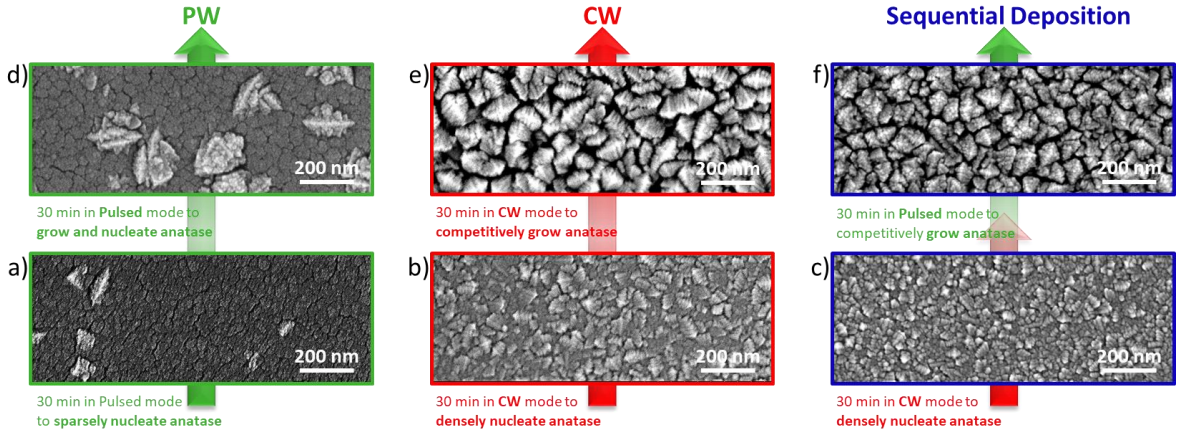

Figure 7 : SEM top-views micrographs of TiO_2 coatings synthesised with PW (a,d), CW (b,e) and sequential deposition (SD) plasma processes (c,f) after 30 min (a,b,c) and 60 min (d,e,f)

One can clearly see that SD deposited coating top surface (Figure 7f) displays a high density of anatase containing crystallites, visually very similar to the coating deposited in CW (Figure 7e). As a confirmation, the main anatase Raman peak (E_g at 144 cm^{-1}) amplitude of the SD layer appears almost equal (83%) to the one synthesised with continuous plasma, indicating that nearly the same amount of anatase is synthesised (Figure 8a). Hence, the photocatalytic activity of SD and CW thin films (Figure 8b) are very close (apparent kinetic constants of 0.17 and 0.18 h^{-1} respectively). Although the amount of anatase appears to have a great influence on photocatalytic properties, various factors such as morphology, porosity, crystals orientation must be considered. In addition, the substrate temperature has been monitored all along the

deposition duration (Figure 8c) for 1h CW, 1h PW process and SD process (30min CW + 30 min PW). As expected, at the beginning of the growth, the temperature of the substrate using SD is following the one of the CW process but after 30 min, when the plasma is switched from CW to PW, the curve inflects to follow the pulsed mode temperature trend. Thus, at the end of the SD process (1h) the final temperature of the substrate reaches 58°C only.

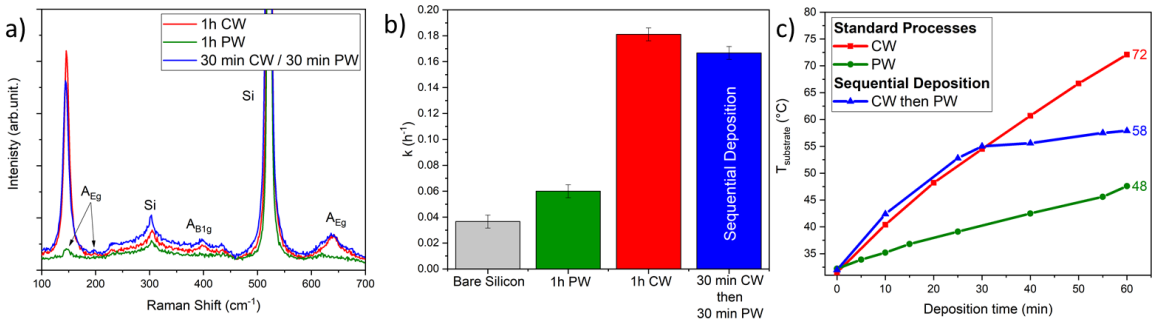

Figure 8 : Raman spectra (a), MB degradation rate under UV (365 nm, 2 mW/cm²) (b) and sample temperature evolution as a function of deposition time (c)

To assess the interest of this combining deposition process, for practical applications, the experimental parameters were adapted to demonstrate its ability for the deposition on a 2 mm thick polycarbonate substrate, denoted PC, (thermal conductivity 0.22 $W.m^{-1}.K^{-1}$). Figure 9 illustrates the major advantages of Sequential Deposition for the deposition of TiO_2 thin films on polycarbonate substrates.

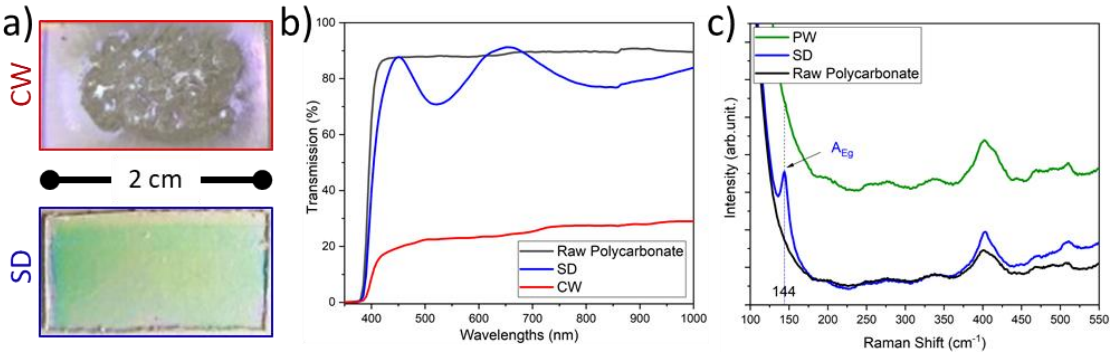

Figure 9 : Pictures of CW and SD coated polycarbonate substrates(a) UV-Vis spectra of raw polycarbonate, SD TiO_2 coated polycarbonate and CW TiO_2 coated polycarbonate (b) and Raman spectra of raw polycarbonate, PW and SD TiO_2 thin film on polycarbonate

Figure 9a presents the top-views of titania films deposited on thick PC substrates in CW and SD deposition mode, respectively. CW mode induced a continuous substrate temperature increase bringing the polycarbonate up to its melting point and therefore strongly degrading its physical properties. On the contrary, polycarbonate coated using the SD process (CW nucleation layer then PW) did not show any degradation. This visual analysis was confirmed by the UV-vis transmission measurements (Figure 9b). Indeed, overall transmission of the CW sample appeared to be around 20% which indicates a major deterioration of the PC optical properties. On the contrary, TiO_2 coated PC substrate using the SD mode displayed only a minor transmission reduction in the visible range, from 90 % to 85 % approximately (oscillations superimposed to the transmission curve for the coated PC are due to interferences within the TiO_2 layer). Besides, Raman scattering did not reveal any anatase evidence in the TiO_2 layer deposited using PW mode only, whereas anatase peak is clearly visible for the TiO_2 coated PC using SD mode (Figure 9c). All these results clearly evidence the advantages provided by the sequential plasma deposition process proposed in this article.

If the interest of the SD method was demonstrated to deposit anatase TiO_2 on thick polycarbonate without damaging the substrate, its functional properties are now discussed (Figure 10). On Figure 10a, the anatase coated PC substrate shows a good ability to degrade methylene blue in aqueous solution under simulated solar irradiation, within a period of 6 h leading to an apparent rate constant degradation of 0.4 h^{-1}. As an illustrative demonstration TiO_2 coated polycarbonate sample was soiled with an artificial sebum to simulate a fingerprint (Artificial Sebum, ASTM D4265-14, Pickering Laboratories) then the coated PC sample was irradiated under the light of a solar simulator. To show the efficiency of the TiO_2 layer, an aluminium foil masked the upper part of the fingerprint during the irradiation time. After 1 hour of exposure, the irradiated part of the fingerprint had nearly completely vanished (Figure 10c). This illustrative example showed the potentialities of this sequential deposition method to

promote for example, a self-cleaning surface on manufacturing products, such as polymeric ophthalmic lenses.

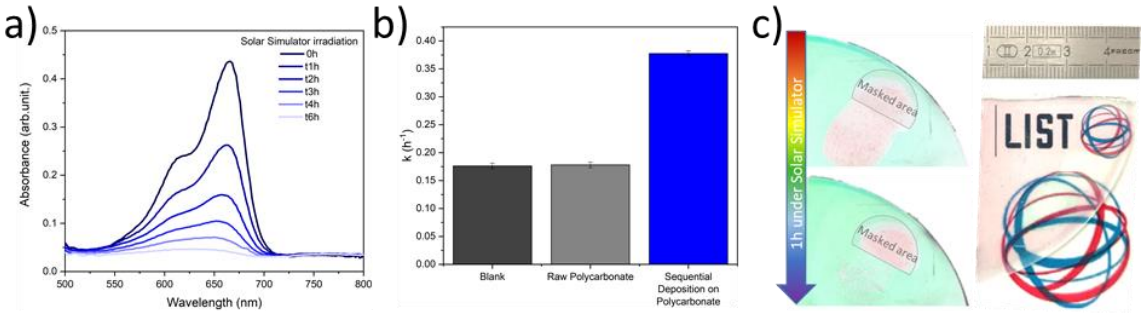

Figure 10 : MB degradation for various solar simulator illumination time (a) rate constant degradation of MB for blank, raw polycarbonate and SD deposited TiO_2 on PC (b) and after/before picture of artificial sebum degradation under sunlight exposure (c)

Whereas conventional Chemical Vapour Deposition can bring up photocatalytic properties to mineral glass substrate at an industrial scale [4] (BIOCLEAN glazing, Saint-Gobain), very few options are available to do the same on polymers. In their review about polymer-supported TiO_2, Singh *et al.* noticed that most of the techniques employed to deposit photocatalytic TiO_2 on polymeric substrates rely on wet chemistry route based on the immobilization of anatase TiO_2 particles via a reasonable heat treatment [13]. These techniques require long deposition or aging time and large amounts of solvents. Knowing the low wettability of polymeric supports, approaches relying on particle immobilization might jeopardize the good adhesion between both raising thus the question of durability and cyclability of such samples. With the perspective of depositing a thin anatase containing layer at rather low substrate temperature, ALD has been shown to be a viable process provided thorough Ti precursor, oxidant and temperature combination (TTiP + H_2O at T_{sub} > 150°C [54], $TiCl_4$ + H_2O at T_{sub} 150°C [55], $TiCl_4$ + H_2O at T_{sub} = 125°C [56]). To decrease the substrate temperature required for anatase nucleation whilst increasing the Growth Per Cycle, plasma enhanced ALD (PEALD) have shown promising results ($TiCl_4$ + O_2/Ar plasma at T_{Sub} = 90°C [57]). Ratzsch *et al.* thoroughly tuned their PEALD settings to deposit anatase containing coating at T_{sub} = 70°C with TTiP + O_2 plasma [54], which is one of the lowest temperature recorded to our knowledge. Although, ALD

process is known to result in very conformal coatings, its growth rate is rather low. For example Ratzsch *et al.* witnessed anatase apparition (sparse hillocks) at 70 °C for coatings of 185 nm [54], obtained after > 5000 cycles with one cycle being 26.530 s, resulting in an overall film deposition duration over 36h. Besides, Physical Vapour Deposition (PVD) techniques also enabled deposition of anatase TiO_2 at low substrate temperature. Zeman *et al.* adapted the total pressure and O_2 partial pressure of their reactive RF magnetron sputtering process to reach anatase at 120°C with a growth rate of 3.2 $nm.min^{-1}$ and a thickness of 250 nm [58]. Zhou *et al.* obtained anatase coating below 75°C with a growth rate ≈ 0.2 $nm.min^{-1}$ with a DC magnetron sputtering reactor [59]. After the optimization of their High Power Impulse Magnetron Sputtering (HiPIMS) process, anatase/rutile layers with photocatalytic activity were deposited on PET and PC substrates by Ratova *et al.*[60]. If HiPIMS appears as a promising mean to deposit rutile and rutile/anatase mixture on thermo labile substrate, the operating window to obtain anatase as the major phase and at a reasonable growth rate seems extremely restricted [61]. Hence, among the different processes allowing the deposition photocatalytic anatase TiO_2 on thermolabile substrate reported in the literature, the process proposed in this manuscript appears attractive as it combines low substrate temperature, decent growth rate and good polymer/TiO_2 adhesion.

4.1 Conclusion

In this article, the morphology and the crystalline structure of different TiO_2 coatings synthesized with a low-pressure radiofrequency (13.56 MHz) **E**lectron **C**yclotron **W**ave **R**esonance PECVD process in continuous and pulsed mode discharges (DC = 50%, 10 kHz) were compared. To do so, different samples with thicknesses ranging from 200 to 900 nm were deposited in both modes and thoroughly characterised. It came out that the plasma discharge mode highly influences the crystalline structure of TiO_2. The continuous wave mode (CW) leads to an entirely covering crystalline top surface after only 30 min of deposition (thickness

of 200 nm) and then, the coating continues to grow following the typical Kolmogorov model. In pulsed wave mode (PW), a thicker incubation layer is required to generate a similar crystallites coverage top surface. Besides, this deposition condition allows to better control the substrate temperature increase and to maintain it below 60°C after 2 hours of plasma deposition. In the second part of this article, the interest of using a deposition method combining the respective advantages of both plasma modes was explored. Hence, the film deposition was split in two steps. The first one, using CW mode, allows a rapid nucleation of anatase nuclei and then, the second step, involving pulsed wave deposition, furthers anatase growth while limiting the heat transferred to the substrate. TiO_2 thin films obtained using this sequential mode exhibited almost equivalent anatase content and similar photocatalytic activity than the coatings obtained in the CW mode, whereas the final substrate temperature was lowered. This sequential deposition mode was successfully applied to deposit a photocatalytic anatase TiO_2 layer on 2 mm thick polycarbonate sheet. Indeed, physical and optical properties of PC sheet remain unaltered thanks to the very limited temperature increase induced by the sequential process (T<60 °C). The photocatalytic activity of such polycarbonate coated sheets has been assessed through MB photodegradation in solution whereas their self-cleaning properties were demonstrated via the vanishing of an artificial sebum fingerprint exposed to a solar simulator. One-hour illumination induced the disappearance of the artificial fingerprint. The proposed process thus appears of major interest for the functionalisation of transparent polymeric sheets that are widely used in practical industrial applications such as polymer lenses and glazing industry. However, it is worth mentioning that the ECWR plasma source (COPRA DN 200 CF, CCR Technology) used for this article is more suited to R&D applications, mainly because of the limited substrate area that can be coated. Indeed, this source provides a plasma beam which allows the deposition of homogenous coating over a surface of 5x5 cm^2. As this ECWR technology can be extended to larger plasma sources and adapted to different shapes, the transfer of this coating solution can be easily implemented. In order to assess the up-scalability

of the proposed process, a semi-industrial pilot line equipped with a larger ECWR plasma source (plasma beam of 120x320 mm) was recently settled in LIST facilities. This new deposition line is also equipped with a roll-to-roll substrate holder allowing the deposition of photocatalytic TiO_2 coatings on larger surfaces in dynamic operation. This development is still on-going and already provided promising results, with the successful deposition of anatase TiO_2 coatings on 300 mm wide roll-to-roll mode. This confirms the potential of the proposed process for industrial applications that would be assessed in future articles.

Acknowledgments

The authors gratefully acknowledge the financial support of the french Agence Nationale de la Recherche (ANR) and luxembourgish Fonds National de la Recherche (FNR) through the FNR-ANR-INTER project PATIO (ANR-17-CE08-0045-01 and INTER/ANR/16/11565003/PATIO/Choquet). The authors gratefully acknowledge the financial support of the french Agence Nationale de la Recherche (ANR) and luxembourgish Fonds National de la Recherche (FNR) through the FNR-ANR-INTER project PATIO (ANR-17-CE08-0045-01 and INTER/ANR/16/11565003/PATIO/Choquet). The help of the prototyping team (Mathieu GERARD and Noureddine BOUSRI) was highly valued and appreciated. We warmly thank the Characterization Platform Pole Leader, Nathalie VALLE, for the constructive discussions about TEM analysis.

Author contributions statement

The manuscript was written with contributions from all authors.

Simon Bulou (S.B.), Mireille Richard-Plouet (M.R.-P.), Agnès Granier (A.G.) Patrick Choquet (P.C.) drafted the project

Benjamin Dey (B.D.), S.B., P.C. planned the experiments

B.D. prepared the coatings and carried out a part of the characterisations and photocalytic tests.

B.D., S.B., P.C. designed and developed the PECVD process.

B.D., William Ravisy (W.R.), M.R.-P., Nicolas Gautier did a part of the characterization analysis.

B.D., S.B., and P.C. analysed the data and wrote the paper.

All authors discussed the results and commented on the paper.

All authors reviewed the manuscript

5.1 References

[1] S. Chaturvedi, P.N. Dave, Environmental application of photocatalysis, Mater. Sci. Forum. 734 (2013) 273–294. https://doi.org/10.4028/www.scientific.net/MSF.734.273.

[2] P. Pichat, Fundamentals of TiO2 Photocatalysis. Consequences for Some Environmental Applications, 2016. https://doi.org/10.1007/978-3-662-48719-8_10.

[3] A. Fujishima, K. Honda, Electrochemical Photolysis of water at a Semiconductor Electrode, Nature. 238 (1972) 38–40. https://doi.org/10.1038/238038a0.

[4] O.M. Ishchenko, V. Rogé, G. Lamblin, D. Lenoble, TiO2- and ZnO-Based Materials for Photocatalysis: Material Properties, Device Architecture and Emerging Concepts, Semicond. Photocatal. - Mater. Mech. Appl. (2016) 3–30. https://doi.org/10.5772/62774.

[5] M. Ge, Q. Li, C. Cao, J. Huang, S. Li, S. Zhang, Z. Chen, K. Zhang, S.S. Al-Deyab, Y. Lai, One-dimensional TiO2 Nanotube Photocatalysts for Solar Water Splitting, Adv. Sci. 4 (2017). https://doi.org/10.1002/advs.201600152.

[6] L.K. Adams, D.Y. Lyon, P.J.J. Alvarez, Comparative eco-toxicity of nanoscale TiO2, SiO2, and ZnO water suspensions, Water Res. 40 (2006) 3527–3532. https://doi.org/10.1016/j.watres.2006.08.004.

[7] E. Baranowska-wójcik, D. Szwajgier, P. Oleszczuk, A. Winiarska-mieczan, Baranowska-Wójcik2020_Article_EffectsOfTitaniumDioxideNanopa.pdf, (2020) 118–129.

[8] I. Iavicoli, V. Leso, A. Bergamaschi, Toxicological effects of titanium dioxide nanoparticles: A review of in vivo studies, J. Nanomater. 2012 (2012). https://doi.org/10.1155/2012/964381.

[9] A. Koltsakidou, Z. Terzopoulou, G.Z. Kyzas, D.N. Bikiaris, D.A. Lambropoulou, Biobased Poly(ethylene furanoate) Polyester/TiO2 Supported Nanocomposites as Effective Photocatalysts for Anti-inflammatory/Analgesic Drugs, Molecules. 24 (2019). https://doi.org/10.3390/molecules24030564.

[10] H. Dong, G. Zeng, L. Tang, C. Fan, C. Zhang, X. He, Y. He, An overview on limitations of TiO2-based particles for photocatalytic degradation of organic pollutants and the corresponding countermeasures, Water Res. 79 (2015) 128–146. https://doi.org/10.1016/j.watres.2015.04.038.

[11] M. Niederberger, M.H. Bartl, G.D. Stucky, Benzyl alcohol and titanium tetrachloride - A versatile reaction system for the nonaqueous and low-temperature preparation of crystalline and luminescent titania nanoparticles, Chem. Mater. 14 (2002) 4364–4370. https://doi.org/10.1021/cm021203k.

[12] J.P. Jolivet, S. Cassaignon, C. Chanéac, D. Chiche, E. Tronc, Design of oxide nanoparticles by aqueous chemistry, J. Sol-Gel Sci. Technol. 46 (2008) 299–305. https://doi.org/10.1007/s10971-007-1645-4.

[13] S. Singh, H. Mahalingam, P.K. Singh, Polymer-supported titanium dioxide photocatalysts for environmental remediation: A review, Appl. Catal. A Gen. 462–463 (2013) 178–195. https://doi.org/10.1016/j.apcata.2013.04.039.

[14] N.M. Ainali, D. Kalaronis, E. Evgenidou, D.N. Bikiaris, D.A. Lambropoulou, Insights into Biodegradable Polymer-Supported Titanium Dioxide Photocatalysts for Environmental Remediation, Macromol. 1 (2021) 201–233. https://doi.org/10.3390/macromol1030015.

[15] Z. Yang, H. Peng, W. Wang, T. Liu, Improved Adhesion of TiO2-Based Multilayer Coating on HDPE and Characterization of Photocatalysis, J. Appl. Polym. Sci. 116 (2010) 2658–2667. https://doi.org/10.1002/app.

[16] R. Portela, Evaluation of several commercial polymers as support for TiO2 in photocatalytic applications, Glob. NEST J. 16 (2018) 525–535. https://doi.org/10.30955/gnj.001446.

[17] M.K. Mishra, S. Chattopadhyay, A. Mitra, G. De, Low temperature fabrication of photoactive anatase TiO2 coating and phosphor from water-alcohol dispersible nanopowder, Ind. Eng. Chem. Res. 54 (2015) 928–937. https://doi.org/10.1021/ie5033028.

[18] V. Miikkulainen, M. Leskelä, M. Ritala, R.L. Puurunen, Crystallinity of inorganic films grown by atomic layer deposition: Overview and general trends, J. Appl. Phys. 113 (2013). https://doi.org/10.1063/1.4757907.

[19] D. Li, S. Dai, A. Goullet, A. Granier, The Effect of Plasma Gas Composition on the Nanostructures and Optical Properties of TiO $_2$ Films Prepared by Helicon-PECVD, Nano. 13 (2018) 1850124. https://doi.org/10.1142/S1793292018501242.

[20] D. Li, N. Gautier, B. Dey, S. Bulou, M. Richard-Plouet, W. Ravisy, A. Goullet, P. Choquet, A. Granier, TEM analysis of photocatalytic TiO2 thin films deposited on polymer substrates by low-temperature ICP-PECVD, Appl. Surf. Sci. 491 (2019) 116–122. https://doi.org/10.1016/j.apsusc.2019.06.045.

[21] Q. Zhang, C. Li, Pure Anatase Phase Titanium Dioxide Films Prepared by Mist Chemical Vapor Deposition, Nanomaterials. 8 (2018) 827. https://doi.org/10.3390/nano8100827.

[22] H. Toku, R.S. Pessoa, H.S. Maciel, M. Massi, U.A. Mengui, The effect of oxygen concentration on the low temperature deposition of TiO2 thin films, Surf. Coatings Technol. 202 (2008) 2126–2131. https://doi.org/10.1016/j.surfcoat.2007.08.075.

[23] H. Nizard, M.L. Kosinova, N.I. Fainer, Y.M. Rumyantsev, B.M. Ayupov, Y. V. Shubin, Deposition of titanium dioxide from TTIP by plasma enhanced and remote plasma enhanced chemical vapor deposition, Surf. Coatings Technol. 202 (2008) 4076–4085. https://doi.org/10.1016/j.surfcoat.2008.02.023.

[24] F. Piallat, C. Vallée, R. Gassilloud, P. Michallon, B. Pelissier, P. Caubet, PECVD RF versus dual frequency: An investigation of plasma influence on metal-organic precursors' decomposition and material characteristics, J. Phys. D. Appl. Phys. 47 (2014). https://doi.org/10.1088/0022-3727/47/18/185201.

[25] L. Youssef, A.J. Kinfack Leoga, S. Roualdes, J. Bassil, M. Zakhour, V. Rouessac, A. Ayral, M. Nakhl, Optimization of N-doped TiO2multifunctional thin layers by low frequency PECVD process, J. Eur. Ceram. Soc. 37 (2017) 5289–5303. https://doi.org/10.1016/j.jeurceramsoc.2017.05.010.

[26] A. Borras, J.R. Sanchez-Valencia, R. Widmer, V.J. Rico, A. Justo, A.R. Gonzalez-Elipe, Growth of crystalline TiO2 by plasma enhanced chemical vapor deposition, Cryst. Growth Des. 9 (2009) 2868–2876. https://doi.org/10.1021/cg9001779.

[27] G.A. Battiston, R. Gerbasi, A. Gregori, M. Porchia, S. Cattarin, G.A. Rizzi, PECVD of amorphous TiO 2 thin films : effect of growth temperature and plasma gas composition, Thin Solid Films. (2000) 126–131. https://doi.org/10.1016/S0040-6090(00)00998-6.

[28] D. Li, M. Carette, A. Granier, J.P. Landesman, A. Goullet, Effect of ion bombardment on the structural and optical properties of TiO<inf>2</inf> thin films deposited from oxygen/titanium tetraisopropoxide inductively coupled plasma, Thin Solid Films. 589

(2015) 783–791. https://doi.org/10.1016/j.tsf.2015.07.015.

[29] Y. Yasuda, K. Kamikuri, M. Tobisaka, Y. Hoshi, Low-temperature deposition of crystallized TiO 2 thin films, Thin Solid Films. 520 (2012) 3736–3740. https://doi.org/10.1016/j.tsf.2011.10.170.

[30] Y. Liu, A. Tang, Q. Zhang, Y. Yin, Seed-Mediated Growth of Anatase TiO2 Nanocrystals with Core-Antenna Structures for Enhanced Photocatalytic Activity, J. Am. Chem. Soc. 137 (2015) 11327–11339. https://doi.org/10.1021/jacs.5b04676.

[31] V.F. Silva, V. Bouquet, S. Députier, S. Boursicot, S. Ollivier, I.T. Weber, V.L. Silva, I.M.G. Santos, M. Guilloux-Viry, A. Perrin, Substrate-controlled allotropic phases and growth orientation of TiO 2 epitaxial thin films, J. Appl. Crystallogr. 43 (2010) 1502–1512. https://doi.org/10.1107/S0021889810041221.

[32] S.C. Jung, S.J. Kim, N. Imaishi, Y.I. Cho, Effect of TiO 2 thin film thickness and specific surface area by low-pressure metal-organic chemical vapor deposition on photocatalytic activities, Appl. Catal. B Environ. 55 (2005) 253–257. https://doi.org/10.1016/j.apcatb.2004.08.009.

[33] J. Yu, X. Zhao, Q. Zhao, Effect of film thickness on the grain size and photocatalytic activity of the sol-gel derived nanometer TiO2thin films, J. Mater. Sci. Lett. 19 (2000) 1015–1017. https://doi.org/10.1023/A:1006705316651.

[34] D. Li, W. Zhang, A. Goullet, Influence of PECVD-TiO2film morphology and topography on the spectroscopic ellipsometry data fitting process, Mod. Phys. Lett. B. 34 (2020). https://doi.org/10.1142/S0217984920502280.

[35] W.G. Lee, S.I. Woo, J.C. Kim, S.H. Choi, K.H. Oh, Preparation and properties of amorphous TiO2 thin films by plasma enhanced chemical vapor deposition, Thin Solid Films. 237 (1994) 105–111. https://doi.org/10.1016/0040-6090(94)90245-3.

[36] M.T. Seman, D.N. Richards, P.C. Rowlette, N.G. Kubala, C.A. Wolden, M.T. Seman, Enhancement of metal oxide deposition rate and quality using pulsed plasma- enhanced chemical vapor deposition at low frequency Enhancement of metal oxide deposition rate and quality using pulsed plasma-enhanced chemical vapor deposition at low frequency, 1213 (2008) 15–20. https://doi.org/10.1116/1.2966425.

[37] B. Dey, S. Bulou, T. Gaulain, W. Ravisy, M.R. Plouet, A. Goullet, A. Granier, Anatase - TiO 2 deposited at low temperature by pulsing an electron cyclotron wave resonance plasma source, Sci. Rep. (2020) 1–11. https://doi.org/10.1038/s41598-020-78956-1.

[38] K. Baba, S. Bulou, M. Quesada-Gonzalez, S. Bonot, D. Collard, N.D. Boscher, P. Choquet, Significance of a Noble Metal Nanolayer on the UV and Visible Light Photocatalytic Activity of Anatase TiO2Thin Films Grown from a Scalable PECVD/PVD Approach, ACS Appl. Mater. Interfaces. 9 (2017) 41200–41209. https://doi.org/10.1021/acsami.7b10904.

[39] M. Weiler, K. Lang, E. Li, J. Robertson, Deposition of tetrahedral hydrogenated amorphous carbon using a novel electron cyclotron wave resonance reactor, Appl. Phys. Lett. 72 (1998) 1314–1316. https://doi.org/10.1063/1.121069.

[40] D. Li, N. Gautier, B. Dey, S. Bulou, M. Richard-Plouet, W. Ravisy, A. Goullet, P. Choquet, A. Granier, TEM analysis of photocatalytic TiO2 thin films deposited on polymer substrates by low-temperature ICP-PECVD, Appl. Surf. Sci. 491 (2019) 116–122. https://doi.org/10.1016/j.apsusc.2019.06.045.

[41] W. Ravisy, M. Richard-Plouet, B. Dey, S. Bulou, P. Choquet, A. Granier, A. Goullet, Unveiling a critical thickness in photocatalytic TiO2thin films grown by plasma-

enhanced chemical vapor deposition using real time in situ spectroscopic ellipsometry, J. Phys. D. Appl. Phys. 54 (2021). https://doi.org/10.1088/1361-6463/ac1ec1.

[42] R. Alcántara, J. Navas, C. Fernández-Lorenzo, J. Martín, E. Guillén, J.A. Anta, Synthesis and Raman spectroscopy study of TiO2 nanoparticles, Phys. Status Solidi Curr. Top. Solid State Phys. 8 (2011) 1970–1973. https://doi.org/10.1002/pssc.201000319.

[43] R. Furushima, S. Tanaka, Z. Kato, K. Uematsu, Orientation distribution-Lotgering factor relationship in a polycrystalline material - As an example of bismuth titanate prepared by a magnetic field, J. Ceram. Soc. Japan. 118 (2010) 921–926. https://doi.org/10.2109/jcersj2.118.921.

[44] G. Liu, H.G. Yang, J. Pan, Y.Q. Yang, G.Q.M. Lu, H.M. Cheng, Titanium dioxide crystals with tailored facets, Chem. Rev. 114 (2014) 9559–9612. https://doi.org/10.1021/cr400621z.

[45] R. Katal, S. Masudy-Panah, M. Tanhaei, M.H.D.A. Farahani, H. Jiangyong, A review on the synthesis of the various types of anatase TiO2 facets and their applications for photocatalysis, Chem. Eng. J. 384 (2020) 123384. https://doi.org/10.1016/j.cej.2019.123384.

[46] S. Liu, J. Yu, M. Jaroniec, Anatase TiO2 with dominant high-energy {001} facets: Synthesis, properties, and applications, Chem. Mater. 23 (2011) 4085–4093. https://doi.org/10.1021/cm200597m.

[47] J. Yu, J. Low, W. Xiao, P. Zhou, M. Jaroniec, Enhanced Photocatalytic CO_2-Reduction Activity of Enhanced Photocatalytic CO_2 -Reduction Activity of Anatase TiO_2 by Co-exposed {001} and {101} Facets, J. Am. Chem. Soc. 136 (2014) 8839.

[48] M.A. Lara, M.J. Sayagués, J.A. Navío, M.C. Hidalgo, A facile shape-controlled synthesis of highly photoactive fluorine containing TiO2 nanosheets with high {001} facet exposure, J. Mater. Sci. 53 (2018) 435–446. https://doi.org/10.1007/s10853-017-1515-6.

[49] X. Niu, Y.E. Du, Y. Liu, H. Qi, J. An, X. Yang, Q. Feng, Hydrothermal synthesis and formation mechanism of the anatase nanocrystals with co-exposed high-energy {001}, {010} and [111]-facets for enhanced photocatalytic performance, RSC Adv. 7 (2017) 24616–24627. https://doi.org/10.1039/c7ra03707d.

[50] M.S. Beato, I. Capua, D. Alexander, From amorphous to microcrystalline silicon: moving from one to the other by halogenated silicon plasma chemistry, 2010.

[51] X. Nie, F. Ma, D. Ma, K. Xu, Thermodynamics and kinetic behaviors of thickness-dependent crystallization in high-k thin films deposited by atomic layer deposition, J. Vac. Sci. Technol. A Vacuum, Surfaces, Film. 33 (2015) 01A140. https://doi.org/10.1116/1.4903946.

[52] K. Kukli, M. Ritala, J. Aarik, T. Uustare, M. Leskelä, Influence of growth temperature on properties of zirconium dioxide films grown by atomic layer deposition, J. Appl. Phys. 92 (2002) 1833–1840. https://doi.org/10.1063/1.1493657.

[53] A. Borrás, J.R. Sánchez-Valencia, J. Garrido-Molinero, A. Barranco, A.R. González-Elipe, Porosity and microstructure of plasma deposited TiO2 thin films, Microporous Mesoporous Mater. 118 (2009) 314–324. https://doi.org/10.1016/j.micromeso.2008.09.002.

[54] S. Ratzsch, E.B. Kley, A. Tünnermann, A. Szeghalmi, Influence of the oxygen plasma parameters on the atomic layer deposition of titanium dioxide, Nanotechnology. 26 (2015) 24003. https://doi.org/10.1088/0957-4484/26/2/024003.

[55] J. Aarik, A. Aidla, H. Mändar, T. Uustare, Atomic layer deposition of titanium dioxide from TiCl4 and H2O: Investigation of growth mechanism, Appl. Surf. Sci. 172 (2001) 148–158. https://doi.org/10.1016/S0169-4332(00)00842-4.

[56] A. Tarre, A. Rosental, V. Sammelselg, T. Uustare, a, Appl. Surf. Sci. 175–176 (2001) 111–116. https://doi.org/10.1016/S0169-4332(01)00051-4.

[57] A. Strobel, H.-D. Schnabel, U. Reinhold, S. Rauer, A. Neidhardt, Room temperature plasma enhanced atomic layer deposition for TiO 2 and WO 3 films , J. Vac. Sci. Technol. A Vacuum, Surfaces, Film. 34 (2016) 01A118. https://doi.org/10.1116/1.4935356.

[58] P. Zeman, S. Takabayashi, Effect of total and oxygen partial pressures on structure of photocatalytic TiO2 films sputtered on unheated substrate, Surf. Coatings Technol. 153 (2002) 93–99. https://doi.org/10.1016/S0257-8972(01)01553-5.

[59] W. Zhou, X. Zhong, X. Wu, L. Yuan, Low temperature deposition of nanocrystalline TiO 2 films : enhancement of nanocrystal formation by energetic, J. Phys. D. Appl. Phys. 40 (2006) 219–226. https://doi.org/10.1088/0022-3727/40/1/018.

[60] M. Ratova, G.T. West, P.J. Kelly, Optimisation of HiPIMS photocatalytic titania coatings for low temperature deposition, Surf. Coatings Technol. 250 (2014) 7–13. https://doi.org/10.1016/j.surfcoat.2014.02.020.

[61] U.H. Felipe Cemin, Makoto Tsukamoto, Julien Keraudy, Vinícius Gabriel Antunes, and D.L. Fernando Alvarez, Tiberiu Minea, Low-energy ion irradiation in HiPIMS to enable anatase TiO2 selective growth, J. Phys. D. Appl. Phys. (2018). https://doi.org/10.1088/1361-6463/aac080.